Science Arts & Métiers (SAM)

is an open access repository that collects the work of Arts et Métiers Institute of Technology researchers and makes it freely available over the web where possible.

This is an author-deposited version published in: https://sam.ensam.eu
Handle ID: .http://hdl.handle.net/10985/25266

To cite this version :

Anthony ROUX, Jennyfer LECOMPTE, Ivan IORDANOFF, Sébastien LAPORTE - Modeling of muscular activation of the muscle-tendon complex using discrete element method - Computer Methods in Biomechanics and Biomedical Engineering, - Vol. 24, n°11, p.1184-1194 - 2021

Any correspondence concerning this service should be sent to the repository Administrator : scienceouverte@ensam.eu

Arts et Métiers Institute of Technology

Modeling of muscular activation of the muscle-tendon complex using discrete element method

Dr. Anthony Roux[a,b], Dr. Jennyfer Lecompte[a], Pr. Ivan Iordanoff[b] and Pr. Sébastien Laporte[a]

[a]Arts et Métiers—Institute of Technology, Institut de Biomécanique Humaine Georges Charpak, LBM, Paris, France; [b]Arts et Métiers—Institute of Technology, I2M Bordeaux, France

ABSTRACT

The tearing of a muscle-tendon complex (MTC) is caused by an eccentric contraction; however, the structures involved and the mechanisms of rupture are not clearly identified. The passive mechanical behavior the MTC has already been modeled and validated with the discrete element method. The muscular activation is the next needed step. The aim of this study is to model the muscle fiber activation and the muscular activation of the MTC to validate their active mechanical behaviors. Each point of the force/length relationship of the MTC (using a parabolic law for the force/length relationship of muscle fibers) is obtained with two steps: 1) a passive tensile (or contractile) test until the desired elongation is reached and 2) fiber activation during a position holding that can be managed thanks to the Discrete Element model. The muscular activation is controlled by the activation of muscle fiber. The global force/length relationship of a single fiber and of the complete MTC during muscular activation is in agreement with literature. The influence of the external shape of the structure and the pennation angle are also investigated. Results show that the different constituents of the MTC (extracellular matrix, tendon), and the geometry, play an important role during the muscular activation and enable to decrease the maximal isometric force of the MTC. Moreover, the maximal isometric force decreases when the pennation angle increases. Further studies will combine muscular activation with a stretching of the MTC, until rupture, in order to numerically reproduce the tearing of the MTC.

KEYWORDS

Muscle-tendon complex; discrete element method; muscular activation; active behavior; fiber

1. Introduction

The tearing of the muscle-tendon complex (MTC), one of the main sport injuries, is caused by an eccentric contraction (Bianchi et al. 2006; Uchiyama et al. 2011). The MTC is a multi-scale material, composed of numerous fascicles gathered together in a conjunctive sheath (epimysium). The Discrete Element Method (DEM) (Cundall and Strack 1979) used for modeling composite materials could be adapted to fibrous and complex materials as the MTC (Brocklehurst et al. 2015; Roux et al. 2016; Audenaert et al. 2019). This method allows to model the complex behavior of the MTC with only simple linear elements. Compared to finite element method using complex mechanical behavior law for muscular activation (Pham et al. 2018; Li et al. 2019), DEM can provide the MTC's behavior with a simple discretization scheme in terms of concept and implementation (André et al. 2012; Roux et al. 2016). DEM model has the advantage of having two scales of studies: the scale of the spherical components (microscopic scale) and the scale of the global behavior of the structure (macroscopic scale) (André et al. 2012). The DEM can explain complex mechanical responses with simple mechanical laws. However, the non-linear properties of the material cannot be introduced easily in the bond properties. DEM can be time-consuming since in DEM simulation, 80% of computing time is spent in searching the particles' contacts and deducing the force acting on the contacts (Iliescu et al. 2010). Further studies will focus on rupture and fiber delamination, which is easy to model with DEM, breaking a single spring between two discrete elements.

The passive behavior of the MTC has already been modeled and validated during a tensile test with the DEM (Roux et al. 2016). Muscular activation is the next step needed to model the complex behavior of the MTC. The active force/length relationship of a MTC describes the evolution of its force for different lengths of the complex, during the fiber activation (Gordon et al. 1966; Woittiez et al. 1983; Goubel and

CONTACT Anthony Roux aroux@crans.org; Sébastien Laporte sebastien.laporte@ensam.eu

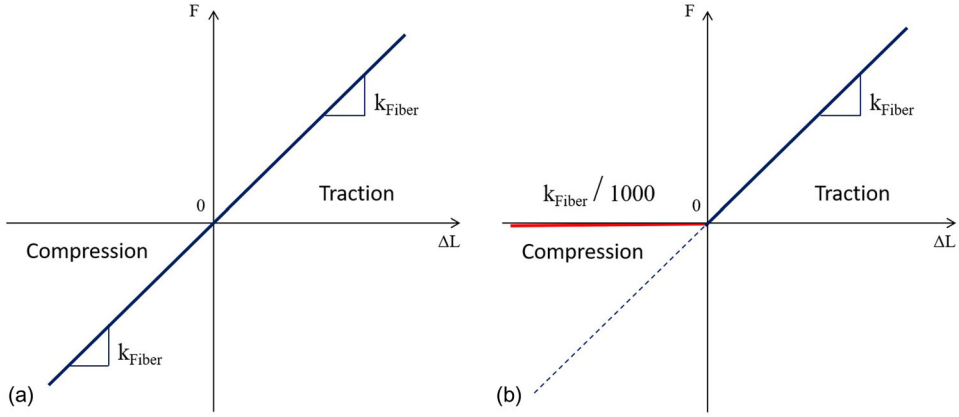

Figure 1. (a) Passive force/length relationship of a spring constituting a muscle fiber (for compressive and tensile mechanical behavior). (b) Modification of the mechanical compressive behavior of the muscle fiber.

Lensel-Corbeil 1998; Winter and Challis 2010; Mohammed and Hou 2016; Rockenfeller and Günther 2018). Knowing the active behavior of a simple muscle fiber will help to understand the global active behavior of the MTC. The different constituents of the MTC (tendon, extra-cellular matrix, …) have an influence on the active behavior of the MTC. Structural effects as the external shape or the pennation angle will also influence the response under active solicitation of the MTC (Gras et al. 2012; Roux et al. 2016). For instance, an increase in the tendon width or the pennation angle, increase the global strain inside the MTC. An opposite effect is noticed with the increase in the muscle width. Moreover, a decrease in the pennation angle of the MTC can be highlighted during a tensile test due to the heterogeneous response of the MTC and the fiber's reorientation during the mechanical solicitation.

In this work, we focus on the feasibility of muscular activation of the MTC using the DEM in 3 D. All our results are then compared with data from the literature.

The aim of this study is first to model the muscle fiber activation and the muscular activation of the MTC using the DEM. Then to apply this model in order to study the influence of the external shape and the pennation angle of the MTC during the muscular activation of the MTC.

2. Materials & methods

2.1. Muscle fiber activation

2.1.1. Compressive behavior of a muscle fiber

The mechanical behavior of a muscle fiber used in Roux et al. (2016) is not representative of its real mechanical behavior and needs to be improved. Indeed, a real muscle fiber has no mechanical response during the compressive test. However, in the model, the stiffness in traction and in compression is the same (Figure 1(a)). To take into account this phenomenon and avoid numerical problems with a stiffness equal to zero, the constitutive law of fibers' springs is modified: a stiffness 1000 times inferior to the traction stiffness is imposed to model the compressive mechanical behavior of the muscle fiber (Figure 1(b)).

2.1.2. Force/length relationship of a muscle fiber

The active force/length relationship of a muscle fiber (Gordon et al. 1966; Woittiez et al. 1983, Goubel and Lensel-Corbeil 1998; Winter and Challis 2010; Winters et al. 2011; Mohammed and Hou 2016; Rockenfeller and Günther 2018) can be modeled as a parabolic curve, (Winter and Challis 2010; Mohammed and Hou 2016) (Figure 2). The equation of this parabolic curve is:

$$\begin{cases} F = \alpha.F_{max}.\left(1 - \left(\frac{\Delta l}{l_c}\right)^2\right) & if \;\; l_c \geq \Delta l \geq -l_c \\ F = 0 & else \end{cases} \quad (1)$$

With α being percentage of fiber activation (activation coefficient), $0 \leq \alpha \leq 1$,

The activation coefficient (α) can vary from 0 (no fiber activation) to 1 (maximal fiber activation). This coefficient enables to report the percentage of muscle fibers used to generate the global activation of the MTC (Huijing 1998). In our model, the activation coefficient represents the level of activation of the MTC because all fibers are activated at the same time (to reduce the time of the numerical simulation).

F_{max} : maximal isometric force of a fiber. Based on the work of Winters and Stark (1988) and preliminary

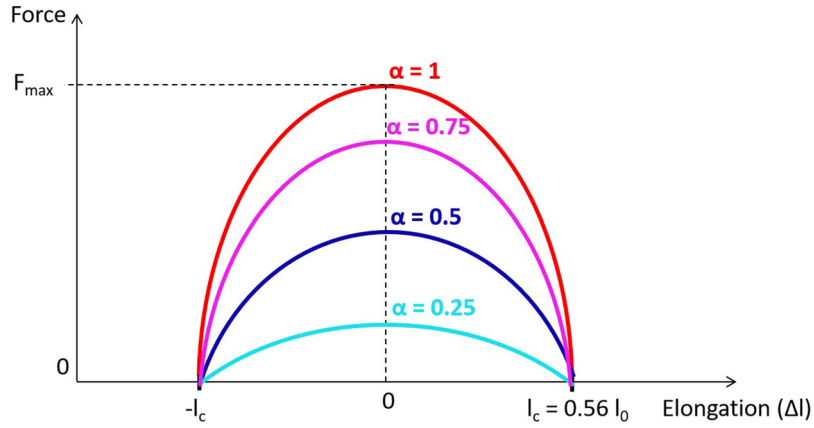

Figure 2. Simplified representation (parabolic curves) of the active force/length relationship, for different levels of activation (α).

studies on the MTC, F_{max} was fixed to 0.3 N for one fiber.

Δl : muscle fiber's elongation,

l_c: characteristic activation length ($l_c = 0.56 \times l_0$) (Gordon et al. 1966; Winters et al. 2011).

l_0: initial length of the muscle fiber. In our model, l_0 is the distance between two spherical discrete elements of the fiber axis (Figure 3(a)).

2.2. Activation of a muscle fiber

To be closer to physiological conditions, fiber extremities are connected to the tendon to test the activation of muscle fibers. The lower part of the tendon extremity is fixed, and a displacement is applied on the upper part of the tendon extremity (Figure 3(a,b)). To anticipate numerical problems linked to the fiber activation, time variation of the activation coefficient is progressive.

A progressive variation of α is chosen to reduce instability problems in the DEM model:

$$\alpha = \alpha_{max} \cdot \frac{1}{2} \cdot \left(1 - \cos\left[\pi \cdot \frac{t}{\Delta t}\right]\right) \qquad (2)$$

With $\alpha_{max} = 1$, Δt = variation's time of α (10 seconds is used for numerically reproduce the fiber activation with the software).

2.3. Definition of the structures and shapes of the MTC

To analyze the influence of the structure on the macroscopic contractile behavior of the global MTC and its maximal isometric force, different structures and shapes are studied: an equivalent MTC with one muscle fiber and tendons at the ends, one parallelepiped equivalent MTC with 400 aligned muscle fibers (with the tendon at the ends and the epimysium on the sides of the structure); one parallelepiped equivalent MTC with 400 angled (20°) muscle fibers; one cylindrical equivalent MTC with 400 angled (20°) muscle fibers; one MTC with a pennation angle of 20° (Figure 4). To use previous results on the tensile response of a MTC, to decrease the computing time and to analyze, as a first step, the phenomenon of muscular activation, the mean dimensions of the MTC are the same as in the previous work by Roux et al. (2016): length of the muscle = 134 mm, length of the tendon = 13.4 mm, width of the muscle = 12.1 mm, width of the tendon = 6.7 mm and pennation angle = 20°. Those dimensions and the size of the discrete elements used to model fibers imposed a total number of 400 fibers. The global length of the MTC and its central cross-sectional area are the same for all specimens previously described.

Moreover, four pennation angles (10°, 20°, 30° and 40°) are tested with the previously studied MTC to analyze the influence of the pennation angle on the contractile effect.

2.4. MTC model

The mechanical properties and structures of the MTC model were described in Roux et al. (2016) (Figure 5). Numerical model was complete in DEM using GranOO software (www.granoo.org). Mechanical properties of MTC were based on values from the literature (Matschke et al. 2013, Regev et al. 2011). Fibers were built with spherical discrete elements, to model the inertia effects, linked by springs, to model the rheological behavior (stiffness was related to Young's modulus: fiber's Young's modulus = 37.44 kPa). Tendon fibers were built in accordance with the arrangement of finger-like muscle fibers, inserted into the muscle to represent the myo-tendinous junction (MTJ) (Roux et al. 2016) (tendon's Young's modulus = 800 MPa, MTJ's Young's modulus = 400 MPa). Links are also created between fibers

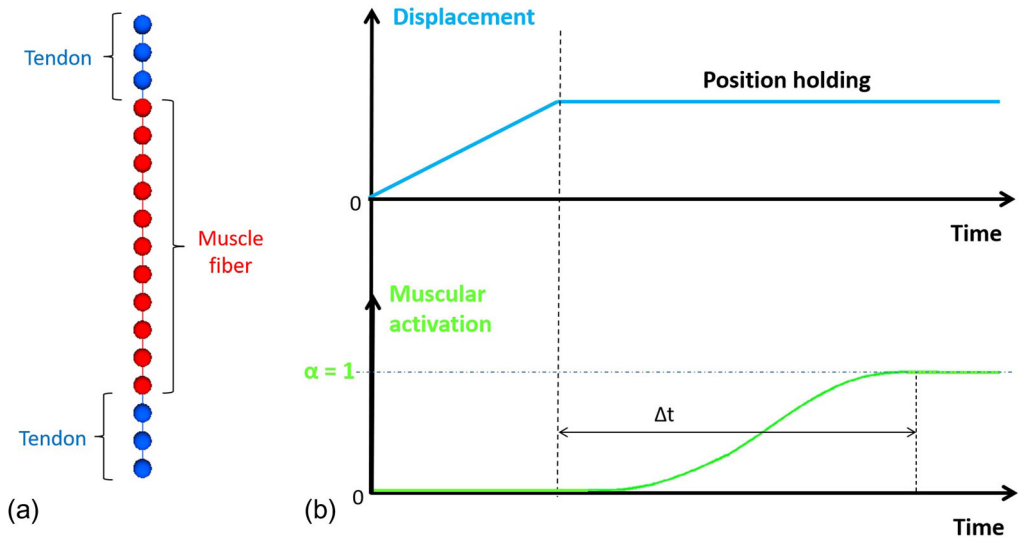

Figure 3. (a) Model of a muscle fiber with its tendon insertions. (b) Sequence composed of an elongation of the muscle fiber followed by position holding with muscle fiber activation.

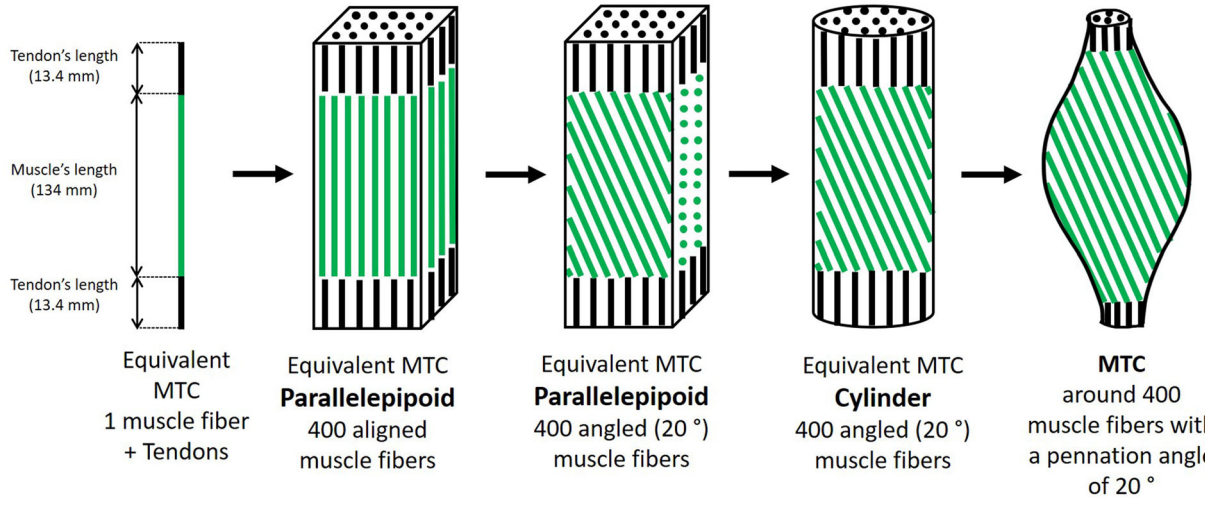

Figure 4. Different studied architectures: from left to right: one equivalent MTC with one muscle fiber and tendons at the extremities; one parallelepiped equivalent MTC with 400 aligned muscle fibers; one parallelepiped equivalent MTC with 400 angled (20°) muscle fibers; one cylindrical equivalent MTC with 400 angled (20°) muscle fibers; one MTC with a pennation angle of 20°.

themselves and between tendon's fibers and the epimysium (same Young's modulus as tendon's fibers) in order to simulate sliding between these two entities. The extracellular matrix (ECM) was computed using springs between fibers in all directions (ECM's Young's modulus = 0.1 MPa). For further information, the reader can refer to Roux et al. 2016.

2.5. Mechanical properties of MTC constituents

To favor muscular activation, the ECM's behavior is modified, decreasing the sliding along of discrete elements of muscle fibers (Figure 6(a,b)). Indeed, during fiber activation, two discrete elements from the same fiber come closer together, favored by the ECM's springs (present in all directions) which enable a sliding along of fiber elements. Increasing the stiffness in compression of the ECM springs is one solution. However, increasing the stiffness of the ECM, located in the longitudinal axis, causes abnormal values of the force during a passive tensile test. Indeed, during a passive tensile test, ECM's springs in the longitudinal axis are compressed since structures are coming closer at the ends of the MTC, linked to the alignment of fibers with the global axis (Roux et al. 2016).

2.6. Boundary conditions

During the numerical test, this active constitutive law (established as a force) is added to the behavior of the

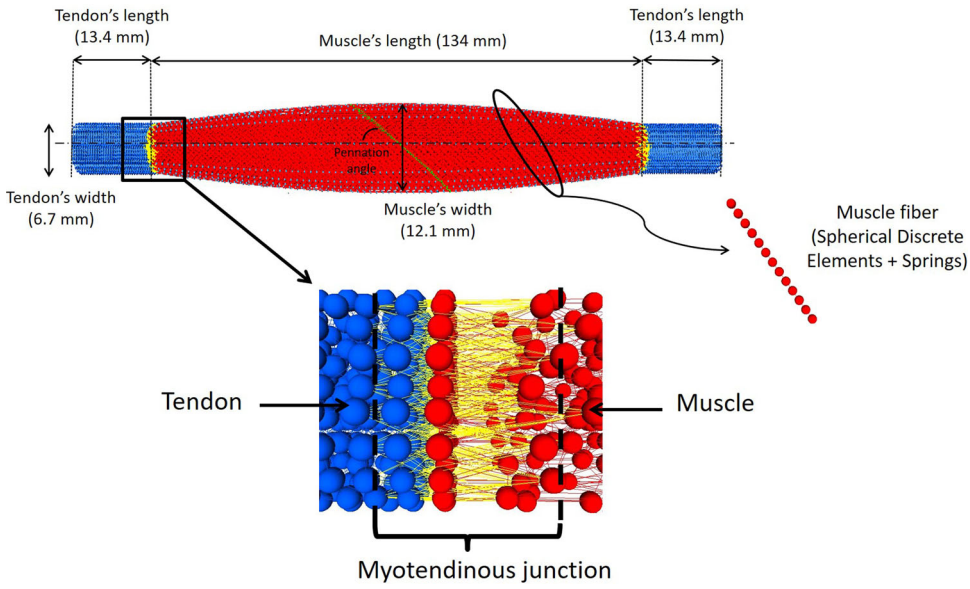

Figure 5. Lateral view of muscle-tendon complex's geometrical parameters and zoom in on the myotendinous junction and on a muscle fiber.

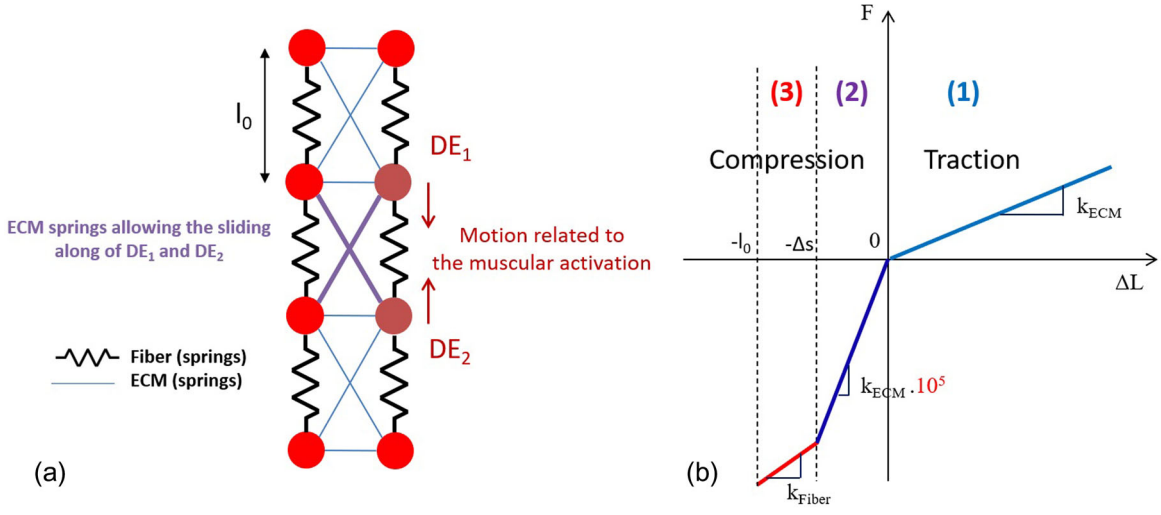

Figure 6. (a). Diagram (in the axis of muscle fiber) of springs of extracellular matrix (ECM) between fibers, allowing the sliding along of the discrete elements during the muscular activation. (b) Modification of the passive force/length relationship of springs of ECM in order to take into account its new compressive behavior. (1) corresponds to the passive behavior in tensile test of the ECM, (2) corresponds to the new compressive behavior of the ECM, allowing the fiber activation and (3) corresponds to the contact between two discrete elements of fibers (Roux et al. 2016).

fiber springs (Roux et al. 2016). The level of activation (α) is the same for all fibers according to the hypothesis which previously established that all MTC's fibers are activated at the same time.

2.7. Data analysis

The force/length relationship is numerically obtained point-to-point for isometric solicitations with a sequence composed of two steps: 1) a passive tensile/compressive test until the desired elongation is reached and 2) fiber activation during a holding in position (Figure 6(b)). The passive force (after the elongation) and the global force (at the end of the sequence) are obtained. The active force is then computed (Factive = Fglobal – Fpassive). Due to a long computing time, this method is applied for every 1% strain and for strain values ranged from −25% to 25% (Winters et al. 2011, Mohammed and Hou 2016, Tomalka et al. 2017, Rockenfeller and Günther 2018).

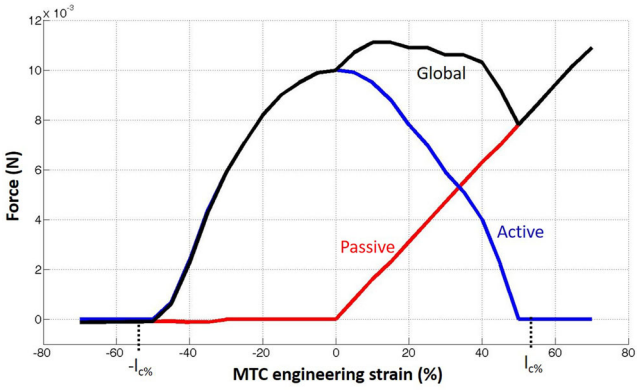

Figure 7. Numerical passive, active and global force/strain relationship of a muscle fiber.

For the first equivalent MTC (with one muscle fiber and tendons), strain values ranged from − 70% to 70% (Winters et al. 2011, Liu et al. 2019), since for this model, the computing time is very low.

The influence of the activation level on the active force of the MTC is also studied. Four values (0.25, 0.5, 0.75 and 1) are chosen to represent the level of activation from low to high muscular activation.

The influence of the structure and external shape of the MTC are also analyzed: the maximal isometric force obtained for each structure previously described, as well as the variation of the pennation angle and the influence of the pennation angle on the passive, active and global force/length relationships for four pennation angles (10°, 20°, 30° and 40°).

3. Results

3.1. Muscle fiber activation

The active force/length relationship of the muscle fiber, akin to a parabolic curve, allows the validation of the activation model and thus leads to the first results on the feasibility of the modeling of muscular activation. The change in the compressive behavior of the muscle fiber leads to consider the relaxation of the muscle fiber during compression.

The aspect of the numerical active force/length curve of the muscle fiber (Figure 7) agrees with the literature (Goubel and Lensel-Corbeil 1998; Winter and Challis 2010; Winters et al. 2011; Mohammed and Hou 2016; Rockenfeller and Günther 2018). At the end of the activation process, the strain is a bit lower than $l_{c\%}$. This simplification of the force/length relationship with a parabolic curve centered in l_0 seems to properly describe the active behavior of the muscle fiber.

3.2. Influence of the structure—Muscular activation of equivalent MTC

The formula of the maximal isometric force (Winters and Stark 1988) enables to obtain an order of magnitude of the maximal isometric force. The maximal isometric force of the equivalent MTC with one fiber and tendons at its ends is 0.3 N, for the parallelepiped equivalent MTC with 400 aligned muscle fibers it is 104.1 N, for the parallelepiped equivalent MTC with 400 angled (20°) muscle fibers, the force is 68.8 N and it is 37.3 N for the cylindrical equivalent MTC with 400 angled (20°) muscle fibers (Figure 8(a)).

3.3. Muscular activation of the MTC

The active behavior of the MTC during the specific sequence of mechanical tests is validated (Figure 8(b)). The global displacement comes to a position holding (2) and the muscle is then activated. The global force (F_{Global}) yielded by the MTC at the end of this specific solicitation is obtained and the active force (F_{Active}) is computed (Figure 8(c)).

The activation level has an influence on the active force of the MTC. The closer α is to 1, the higher is the summit of the parabolic curve (Figure 8(d)). The aspect and the order of curves agree with theoretical results for different activation levels.

The global visualization of the progressive muscular activation is analyzed. For muscular activation after an imposed stretching, the MTC is first stretched and then, for a fixed strain, the MTC is progressively activated until reaching the maximal contraction (Figure 9(a,b)). Numerically, the pennation angle decreases during the muscular activation in isometric or eccentric state (Figure 9(c,d)).

The influence of pennation angles (10°, 20°, 30° and 40°) on the mechanical behavior of the MTC agrees with the literature (Woittiez et al. 1983; Gareis et al. 1992). A decrease in the maximal isometric force is observed when the pennation angle increases (Figure 10(a)–(d)). For a small pennation angle, the force/length relationship is not strictly monotonic; its active behavior has an area of smaller activity, creating an inflexion point on the global force/length curve (Woittiez et al. 1983; Gareis et al. 1992; Tomalka et al. 2017; Liu et al. 2019).

4. Discussion

4.1. Muscle fiber activation

The compressive behavior of the muscle fiber, negligible compared to the tensile stiffness, is implemented

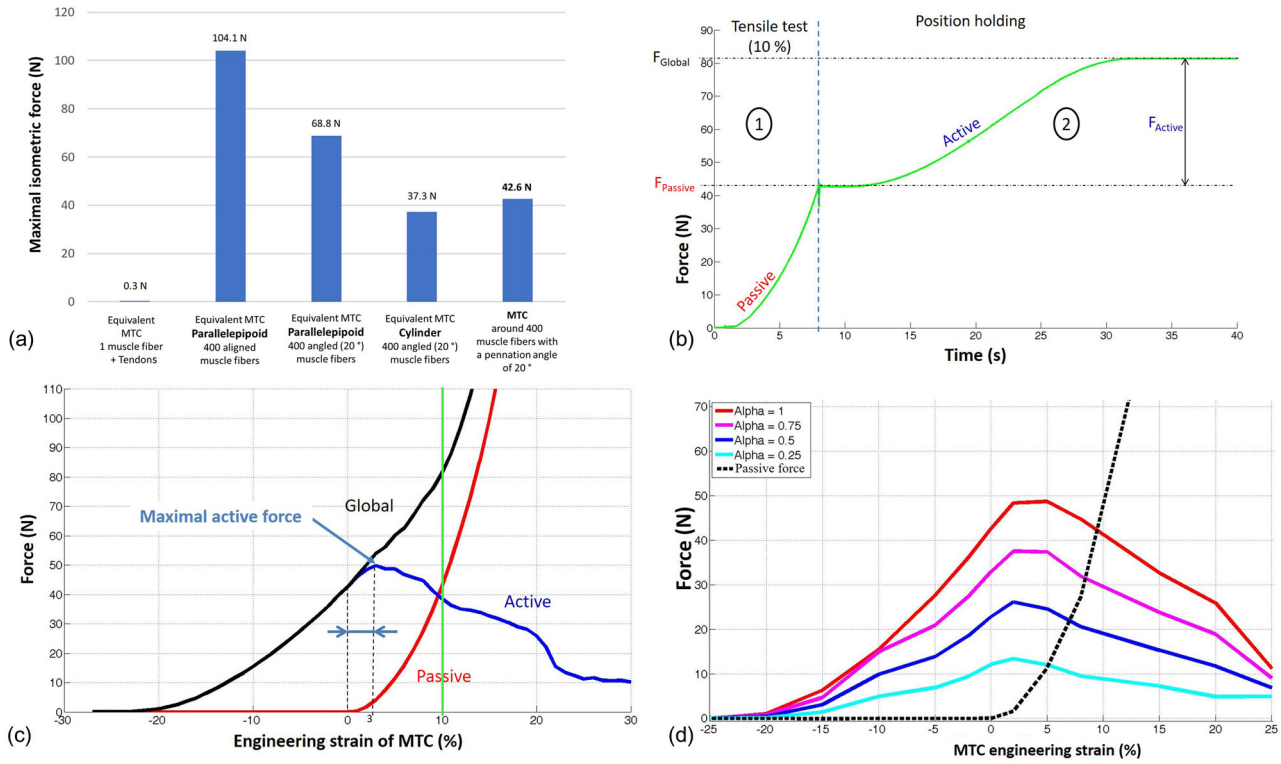

Figure 8. (A) Maximal isometric force for the different equivalent MTC. (b). Example of muscle-tendon complex's (MTC) (with a pennation angle of 20°) force versus time curve for a position holding at 10% of global strain (1) and then muscular activation (2). (c) Active, passive and global force/length curve of the MTC (with a pennation angle of 20°). (d) Active force/length relationship of the muscle-tendon complex (with a pennation angle of 20°) for different activation levels (α).

in the calculation code to prevent problems of numerical instability. Therefore, this new and quasi-null compressive stiffness does not modify the behavior of the fibers and the global behavior of the MTC during simulations. The influence of the ECM on the muscular activation is also important during the displacement of the activated muscle fiber because the ECM is linked to the shearing forces taken by the ECM (Sànchez et al. 2014, Todros et al. 2020).

The parabolic curve was already used to simplify the active force/length relationship (Winter and Challis 2010; Mohammed and Hou 2016). In our study, its value was fixed to 56%, in agreement with reported values on frog legs (Gordon et al. 1966) and reported values on rabbit muscles (Winter and Challis, 2010). This value was chosen because the characteristic activation length is not the same for all MTC: it can vary from 10 to 60% of the MTC's initial length, depending on the type of MTC and its function in the human body (Gordon et al. 1966; Goubel and Lensel-Corbeil 1998; Winter and Challis 2010; Stålhand and Holzapfel 2016).

The overestimation of active force/length curve by DEM compared to theory can be due to the model design and the simplification of the number of constituents of the MTC (ECM, MTJ, epymisium, …). In our model, the muscle fiber is linked, at both extremities, by tendon fibers. This causes a little variation of the global stiffness of the structure and causes some variations on the global strain determination. If the structure is considered as a spring of muscle fiber, linked at each end by a spring of tendon (Figure 6(a)); the global stiffness is: $K_{tot} = \frac{K_t.K_f}{K_t+2.K_f}$ with K_t: the tendon's stiffness, K_F: the muscle fiber's stiffness.

Therefore, the force inside the structure is: $F = \frac{K_t.K_f}{K_t+2.K_f}\Delta l_f + \frac{2.K_t.K_f}{K_t+2.K_f}\Delta l_t$ with Δl_f : muscle fiber's elongation, Δl_t : tendon fiber's elongation.

As the tendon's stiffness is considered superior to the muscle fiber's stiffness ($K_t \gg K_f$), the force is equal to $F = K_f.\Delta l_f + 2.K_t.\Delta l_t$. Therefore, the error between the numerical and the theoretical curve, concerning the strain, is due to the approximation done between K_f and the ratio $\frac{K_t.K_f}{K_t+2.K_f}$.

4.2. Influence of the structure—Muscular activation of equivalent MTC

The influence of the external shape on the maximal isometric force can be related to the influence of

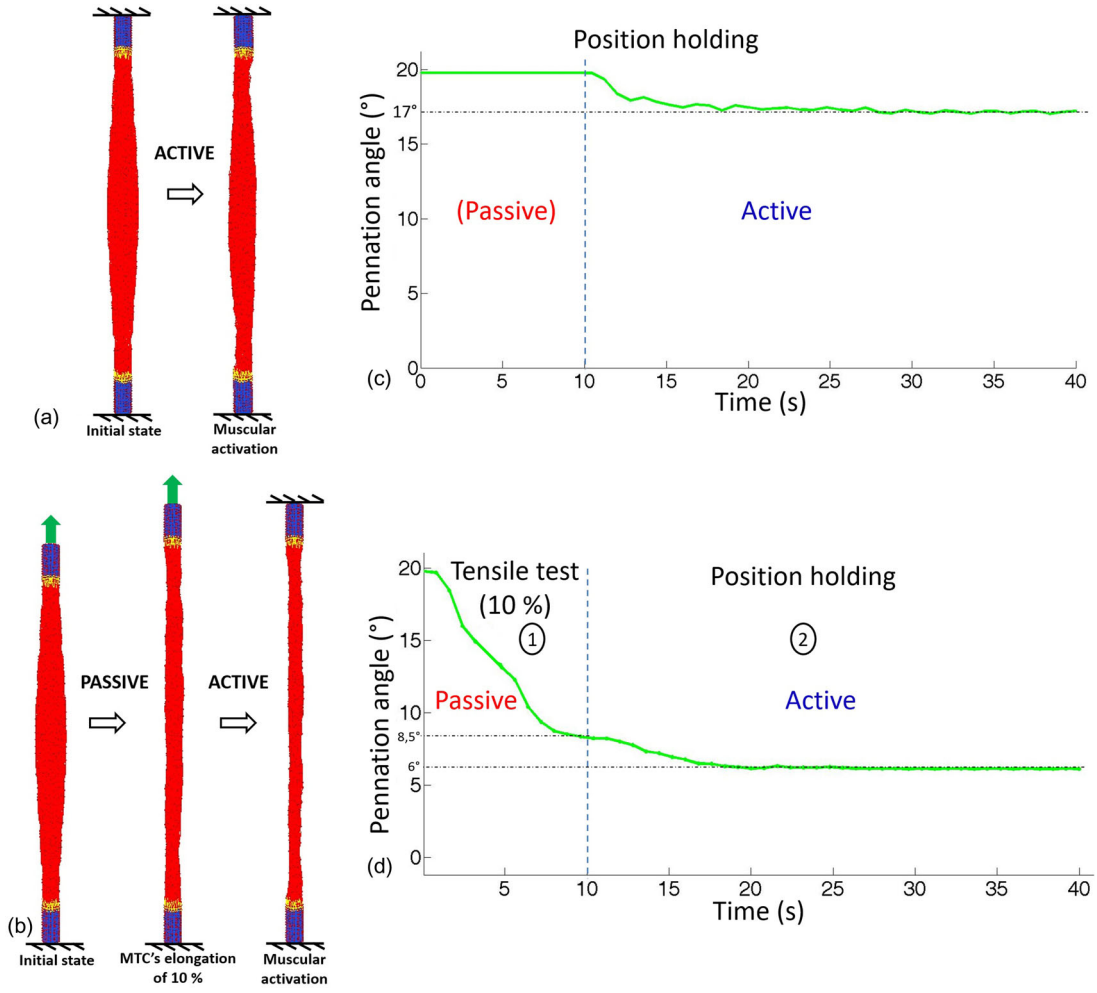

Figure 9. (a) Visualization of the muscle-tendon complex (MTC) during an isometric muscular activation. (b). Visualization of the MTC during the muscular activation for an imposed displacement. From left to right: initial state; passive tensile test until a global strain of 10%; holding in position with muscular activation. (c). Variation of the pennation angle of the MTC during muscular activation in a holding in position. (d). Variation of the pennation angle of the MTC during a passive tensile test until 10% of strain (1) and during muscular activation in a position holding (2).

morphological parameters on the global mechanical behavior during a passive tensile test (Roux et al. 2016). Indeed, for more inclined muscle fibers, the generated force is less oriented on the equivalent MTC's axis. This can be explained by the influence of the pennation angle on the global force of the MTC because the existing relation between the PCSA and the CSA can also be used for the force: $F_{MTC} = F_{Fiber}.\ \cos(Pennation\ Angle)$.

With a maximal isometric force of a muscle fiber fixed at $F_{max\ fiber} = 0.3\,N$, a pack of 400 muscle fibers create a maximal isometric force of $400 \times 0.3 = 120\,N$. However, a parallelepiped of 400 muscle fibers gives a maximal isometric force of 104.2 N and a parallelepiped of 400 muscle fibers oriented by 20° gives a maximal isometric force of 68.8 N. The decrease in force is due to the parallelepiped structure, the pennation angle and the influence of the ECM on the mechanical behavior. For a cylindrical structure with the same dimensions (pennation angle = 20°), the maximal isometric force is 37.3 N. This new decrease is linked to the cylindrical geometry and shorter muscle fibers at the external surface of this specific shape. The relationship between the maximal isometric force of the muscle fiber alone and the equivalent MTC of 400 pennate muscle fibers is not obvious; it depends on the behavior of the ECM, the shape of the equivalent MTC and the value of the pennation angle (Winters and Stark 1988; Winter and Challis 2010; Sànchez et al. 2014; Todros et al. 2020).

Differences can also be linked to the influence of the epimysium which contributes to the global mechanical behavior of the MTC (Roux et al. 2016; Schenk et al. 2020). This sheath is not present on the equivalent MTC model; therefore the active behavior of the MTC is changed.

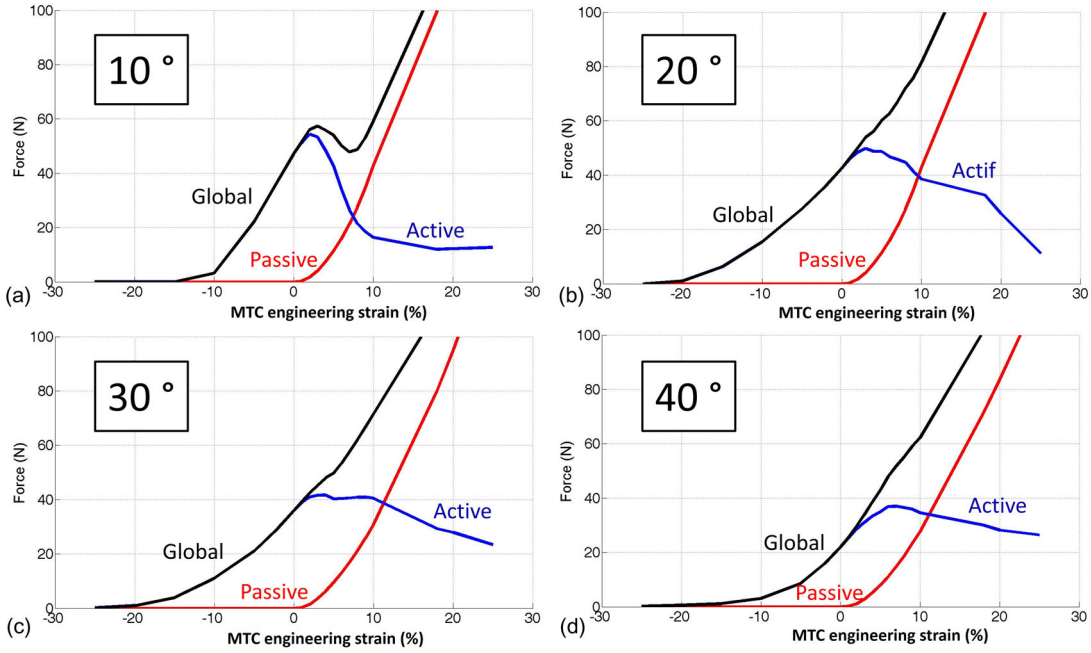

Figure 10. Active, passive and global force/length relationship for the same muscle-tendon complex with different pennation angles. (a) Pennation angle of 10°. (b). Pennation angle of 20°. (c) Pennation angle of 30°. (d). Pennation angle of 40°.

4.3. Muscular activation of the MTC

In our model, all muscle fibers are simultaneously activated during the muscular activation. Anatomically, some areas are under muscular activation according to the required level of activation of the MTC (Kääriäinen et al. 2000; Hedenstierna et al. 2008; Hodgson et al. 2012; Turrina et al. 2013). This model of activation leads to qualitative results on muscular activation but further studies will implement activation's areas to be closer to anatomical descriptions. The modification of the activation level (when other parameters are fixed) can enable increasing or decreasing the muscle activity of the MTC. This can be an alternative way to the simultaneous activation of muscle fibers and could represent the activation of some packs of fibers.

A gap appears between the null strain and the strain at the maximal active force: the maximal active force of the MTC does not appear for a null strain but for a strain value of 3% (Figure 8(c)). This difference can be explained by the pennation angle: Woittiez et al. showed that for similar typological MTC from rats, a difference of the force/length relationship appears between pennate and fusiform muscles (Woittiez et al. 1983, 1984).

The pennation angle decreases during the muscular activation (Figure 10), contrary to many *in vivo* studies (Maganaris et al. 2001; Abellaneda et al. 2009; Narici et al. 2011; Tilp et al. 2011; Simoneau et al. 2012; Vieira et al. 2018). Indeed, during muscular activation, muscle fibers shorten. To increase the force created by the muscle and to transmit the effort through the tendons, muscle fibers will orientate and increase the pennation angle. This increase in pennation angle (5° to 7°), is close to the literature (Narici et al. 2011; Tilp et al. 2011; Schenk et al. 2020). During numerical muscular activation tests, the decrease in the pennation angle ranges around 3° (Figure 9(d)). This result is confirmed by a few studies showing that during an active stretching of the MTC, the muscle fibers' length increases and the pennation angle decreases (Finni et al. 2003; Chino et al., 2008; Tilp et al. 2011). The numerical simulation confirms that during an active stretching, a competition exists between the decrease in the pennation angle linked to the passive stretching and the increase in the pennation angle linked to the muscular activation. Indeed, in our model, this competition appears because fibers are modeled with simple springs for which the displacement can lead to a lengthening or shortening of the muscle.

The difference between force/length relationships can be due to the conjunctive tissue (Wilkie 1968; Huijing et al. 1994; Schenk et al. 2020), to the pennation angle (Figure 10) (Woittiez et al. 1983; Winters and Stark 1988; Gareis et al. 1992; Winter and Challis 2010), to the proportion of slow fibers and to the function of the MTC (Gareis et al. 1992; Tomalka et al. 2017; Eng et al. 2019). Moreover, for pennate MTC, muscle fibers are shorter compared to the

length of the MTC, and by comparison with fusiform muscles. The effect of the modification of the muscle external length on the production of muscle fibers is therefore more pronounced for a muscle with parallel fibers (Gans and Bock 1965).

5. Conclusion

A DEM model of the muscular activation of the MTC has been studied. The active mechanical behavior of the MTC is implemented at the muscle fiber's level. It depends on the role of the ECM, on the external shape of the structure which enable to decrease the maximal isometric force of the MTC. The increase of the pennation angle also has an influence since its increases cause a decrease in the maximal isometric force. Moreover, a relationship is found between the maximal isometric force of one muscle fiber and the one of the MTC. This model of activation leads to qualitative results on muscular activation but further studies will be led to come closer to anatomical descriptions. To obtain a more realistic model, some hypotheses could be improved: the aspect of the force/length relationship, the difference between the types of fibers (fast or slow fibers), the creation of areas of activation.

The next step will consist in combining a muscular activation with a stretching of the MTC, until rupture, to numerically reproduce the tearing of the MTC.

Disclosure statement

No potential conflict of interest was reported by the author(s).

References

Abellaneda S, Guissard N, Duchateau J. 2009. The relative lengthening of the myotendinous structures in the medial gastrocnemius during passive stretching differs among individuals. J Appl Physiol. (1985). 106(1):169–177.

André D, Iordanoff I, Charles J-l, Néauport J. 2012. Discrete element method to simulate continuous material by using the cohesive beam model. Comp Methods Appl Mech Eng. 213–216:113–125.

Audenaert EA, Khanduja V, Bauwens C, Van Hoof T, Pattyn C, Steenackers G. 2019. A discrete element model to predict anatomy of the psoas muscle and path of the tendon: design implications for total hip arthroplasty. Clin Biomech. 70:186–191.

Bianchi S, Poletti P-A, Martinoli C, Abdelwahab IF. 2006. Ultrasound appearance of tendon tears. part 2: lower extremity and myotendinous tears. Skeletal Radiol. 35(2): 63–77.

Brocklehurst P, Adeniran I, Yang D, Sheng Y, Zhang H, Ye J. 2015. A 2D electromechanical model of human atrial tissue using the discrete element method. Biomed Res Int. 2015:854953Volume Article ID 854953

Chino K, Oda T, Kuri Hara T, Nagayoshi T, Yoshikawa K, Kanehisa H, Fukunaga T, Fukashiro S, Kawakami Y. 2008. In vivo fascicle behavior of synergistic muscles in concentric and eccentric plantar flexions in humans. J Electromyogr Kinesiol. 18(1):79–88.

Chino K, Oda T, Kuri Hara T, Nagayoshi T, Yoshikawa K, Kanehisa H, Fukunaga T, Fukashiro S, Kawakami Y. 2008. In vivo fascicle behavior of synergistic muscles in concentric and eccentric plantar flexions in humans. J Electromyogr Kinesiol. 18(1):79–88.

Cundall PA, Strack ODL. 1979. A discrete numerical model for granular assemblies. Géotechnique. 29(1):47–65.

Eng CM, Konow N, Tijs C, Holt NC, Biewener AA. 2019. In vivo force-length and activation dynamics of two distal rat hindlimb muscles in relation to gait and grade. J Exp Biol. 222(24):jeb205559.

Finni T, Ikegawa S, Lepola V, Komi PV. 2003. Comparison of force-velocity relationships of vastus lateralis muscle in isokinetic and in stretch-shortening cycle exercises . Acta Physiol Scand. 177(4):483–491.

Gans C, Bock WJ. 1965. The functional significance of muscle architecture a theoretical analysis. Ergeb Anat Entwicklungsgesch. 38:115–142.

Gareis H, Moshe S, Baratta R, Best R, D'Ambrosia R. 1992. The isometric length-force models of nine different skeletal muscles. J. Biomech. 25 (8):903–916.

Gordon AM, Huxley AF, Julian FJ. 1966. The variation in isometric tension with sarcomere length in vertebrate muscle fibres. J Physiol. 184(1):170–192.

Goubel F, Lensel-Corbeil G. 1998. Biomécanique: Elements de mécanique musculaire. Paris, France: MASSON.

Gras L-L, Mitton D, Viot P, Laporte S. 2012. Hyper-elastic properties of the human sternocleidomastoideus muscle in tension. J Mech Behav Biomed Mater. 15:131–140.

Hedenstierna S, Halldin P, Brolin K. 2008. Evaluation of a combination of continuum and truss finite elements in a model of passive and active muscle tissue. Comput Methods Biomech Biomed Engin. 11(6):627–639.

Hodgson JA, Chi S-W, Yang JP, Chen J-S, Edgerton VR, Sinha S. 2012. Finite element modeling of passive material influence on the deformation and force output of skeletal muscle. J Mech Behav Biomed Mater. 9:163–183.

Huijing PA. 1998. Muscle, the motor of movement: properties in function, experiment and modelling. J Electromyogr Kinesiol. 8(2):61–77.

Huijing PA, Nieberg SM, Vd Veen EA, Ettema GJ. 1994. A comparison of rat extensor digitorum longus and gastrocnemius medialis muscle architecture and length-force characteristics. Acta Anat (Basel). 149(2):111–20.

Iliescu D, Gehin D, Iordanoff I, Girot F, Gutiérrez M. 2010. A discrete element method for the simulation of CFRP cutting. Compos Sci Technol. 70(1):73–80.

Kääriäinen M, Järvinen T, Järvinen M, Rantanen J, Kalimo H. 2000. Relation between myofibers and connective tissue during muscle injury repair. Scand J Med Sci Sports. 10(6):332–337.

Li J, Lu Y, Miller SC, Jin Z, Hua X. 2019. Development of a finite element musculoskeletal model with the ability to predict contractions of three-dimensional muscles. J Biomech. 94 (2019):230–234.

Liu H, Prot VE, Skallerud BH. 2019. Soft palate muscle activation: a modeling approach for improved understanding of obstructive sleep apnea. Biomech Model Mechanobiol. 18(3):531–546.

Maganaris CN, Kawakami Y, Fukunaga T. 2001. Changes in aponeurotic dimensions up on muscle shortening: in vivo observations in man. J Anat. 199(4):449–456.

Matschke V, Jones JG, Lemmey AB, Maddison PJ, Thom JM. 2013. Patellar tendon properties and lower limb function in rheumatoid arthritis and ankylosing spondylitis versus healthy controls: a cross-sectional study. ScientWorld J. 2013:514743

Mohammed GA, Hou M. 2016. Optimization of Active Muscle Force-Length Models Using Least Squares Curve Fitting. IEEE Trans Biomed Eng. 63(3):630–635.

Narici MV, Flueck M, Koesters A, Gimpl M, Reifberger A, Seynnes OR, Niebauer J, Rittweger J, Mueller E. 2011. Skeletal muscle remodeling in response to alpine skiing training in older individuals. Scand J Med Sci Sports. 21 (Suppl 1):23–28.

Pham N, Xue Q, Zheng X. 2018. Coupling between a fiber-reinforced model and a Hill-based contractile model for passive and active tissue properties of laryngeal muscles: a finite element study. J Acoust Soc Am. 144(3):EL248

Regev GJ, Kim CW, Tomiya A, Lee YP, Ghofrani H, Garn SR, Lieber RL, Ward SR. 2011. Psoas muscle architectural design, in vivo sarcomere length range, and passive tensile properties support its role as a lumbar spine stabilizer. Spine (Phila Pa 1976). 36(26):E1666–E1674.

Rockenfeller R, Günther M. 2018. Inter-filament spacing mediates calcium binding to troponin: a simple geometric-mechanistic model explains the shift of force-length maxima with muscle activation. J Theor Biol. 7454: 240–252.

Roux A, Laporte S, Lecompte J, Gras L-L, Iordanoff I. 2016. Influence of muscle-tendon complex geometrical parameters on modeling passive stretch behavior with the discrete element method. J Biomech. 49(2):252–258.

Sànchez C, Lloyd JE, Fels S, Abolmaesumi P. 2014. Embedding digitized fibre fields in finite element models of muscles. Comput Methods Biomech Biomed Eng Imaging Vis. 2(14):223–236. Volume Issue

Schenk P, Papenkort S, Böl M, Siebert T, Grassme R, Rode C. 2020. A simple geometrical model accounting for 3D muscle architectural changes across muscle lengths. J Biomech. 103:109694.

Simoneau EM, Longo S, Seynnes OR, Narici MV. 2012. Human muscle fascicle behavior in agonist and antagonist isometric contractions. Muscle Nerve. 45(1):92–99.

Stålhand J, Holzapfel GA. 2016. Length adaptation of smooth muscle contractile filaments in response to sustained activation. J Theor Biol. 397:13–21.

Tilp M, Steib S, Schappacher-Tilp G, Herzog W. 2011. Changes in fascicle lengths and pennation angles do not contribute to residual force enhancement/depression in voluntary contractions. J Appl Biomech. 27(1):64–73.

Todros S, de Cesare N, Concheri G, Natali AN, Pavan PG. 2020. Numerical modelling of abdominal wall mechanics: The role of muscular contraction and intra-abdominal pressure. J Mech Behav Biomed Mater. 103:103578

Tomalka A, Rode C, Schumacher J, Siebert T. 2017. The active force-length relationship is invisible during extensive eccentric contractions in skinned skeletal muscle fibres. Proc. R. Soc. B 284, pii: 20162497.

Turrina A, Martínez-Gonzâlez MA, Stecco C. 2013. The muscular force transmission system: role of the intramuscular connective tissue. J Bodyw Mov Ther. 17(1): 95–102.

Uchiyama Y, Miyazaki S, Tamaki T, Shimpuku E, Handa A, Omi H, Mochida J. 2011. Clinical results of a surgical technique using endobuttons for complete tendon tear of pectoralis major muscle: report of five cases. Sports Medicine, Arthroscopy, Rehabilitation, Therapy, Technology. 3:20.

Vieira A, Blazevich A, Souza N, Celes R, Alex S, Tufano JJ, Bottaro M. 2018. Acute changes in muscle thickness and pennation angle in response to work-matched concentric and eccentric isokinetic exercise. Appl Physiol Nutr Metab. 43(10):1069–1074.

Wilkie DR. 1968. Muscle. London: Clowes and Sons.

Winter SL, Challis JH. 2010. The expression of the skeletal muscle force-length relationship in vivo: a simulation study. J Theor Biol. 262(4):634–643.

Winters JM, Stark L. 1988. Estimated mechanical properties of synergistic muscles involved in movements of a variety of human joints. J Biomech. 21(12):1027–1041.

Winters TM, Takahashi M, Lieber RL, Ward SR. 2011. Whole muscle length-tension relationships are accurately modeled as scaled sarcomeres in rabbit hindlimb muscles. J Biomech. 44(1):109–115.

Woittiez RD, Huijing PA, Rozendal RH. 1983. Influence of muscle architecture on the length-force diagram of mammalian muscle. Pflugers Arch. 399(4):275–279.